Mesomorphic State of Poly(vinylpyridine)–Dodecylbenzenesulfonic Acid Complexes in Bulk and in Xylene Solution

Olli Ikkala, Janne Ruokolainen, and Gerrit ten Brinke*,†

Department of Technical Physics, Helsinki University of Technology, FIN-02150 Espoo, Finland

Mika Torkkeli and Ritva Serimaa

Department of Physics, Helsinki University, P.O. Box 9, FIN-00140 Helsinki, Finland

Received May 12, 1995; Revised Manuscript Received July 5, 1995®

ABSTRACT: Theoretically, lyotropic behavior of flexible polymers can be induced by associating the polymers with a large amount of long-tail surfactants leading to *bottle–brush* type conformations in suitable solvents. To address this and related questions, complexes of poly(2-vinylpyridine) (P2VP) and poly(4-vinylpyridine) (P4VP) with *p*-dodecylbenzenesulfonic acid (DBSA), characterized by FT-IR, were investigated in the bulk and in xylene, i.e., a good solvent for the alkyl side chains. At a 1:1 molar ratio of vinylpyridine monomer and DBSA, the polymers are shown by FT-IR to be almost completely protonated. In the bulk, the complexes form mesomorphic layer structures which have been characterized by polarized optical microscopy and by both wide- and small-angle X-ray scattering. In the xylene solutions, birefringence indicating liquid crystallinity is observed for concentrations of the fully protonated P4VP-$(DBSA)_{1.0}$ complex of ca. 50% (w/w) and higher. In contrast, for P2VP$(DBSA)_{1.0}$, this is only observed at complex concentrations of ca. 70% (w/w) and higher. The mesomorphic behavior of P4VP$(DBSA)_{1.0}$ in xylene was further demonstrated by SAXS.

Introduction

In the recent literature[1,2] dealing with conductive polymer blends based on polyaniline (PANI), several remarkable observations are made: solutions of PANI protonated with camphorsulfonic acid (CSA) in *m*-cresol show liquid crystalline behavior, and blends of PANI-$(CSA)_{0.5}$ with PMMA (among others) cast from *m*-cresol show a fractal electrically conducting interpenetrating network at concentrations of the complex as low as 1% (w/w). The physical principles underpinning this latter observation are a combination of the interfacial activity of CSA with respect to PMMA, with a corresponding slow phase separation dynamics,[3,4] and the low percolation threshold of objects with a high aspect ratio.[5] Although these phenomena have been amply characterized, relatively few molecular level explanations have been offered. In a recent publication[6] we have demonstrated the role of CSA in combination with phenols. In this case the hydrogen-bonding group in the solvent can associate to the carbonyl group of CSA. A cyclically associated species is formed, in which the phenyl rings in PANI and *m*-cresol interact through van der Waals forces and the phenyl ring of the *m*-cresol molecule takes up a position on top of the PANI ring. The steric combination of interactions yields, among other things, high enough solubility and therefore the relatively stiffened protonated PANI chains exhibit lyotropic behavior in solution and planar conformations in solid films where the solvent has been removed. This molecular recognition type mechanism is quite specific to the polymer, the counterion, and the solvent, and the realization of similar properties in other polymers along this line is not obvious, especially in the case of more flexible polymers.

Fredrickson[7] recently suggested an alternative route also based on surfactants to yield liquid crystalline solutions. In this case essential use is made of the excluded-volume repulsion between the side-chain surfactants, provided that the polymer–surfactant complex is in a good solvent of the side chains. The surfactant molecules are of the amphiphilic type with a polar head and a long flexible tail. The polar head is assumed to associate strongly to a complementary group of the polymer. According to his analysis, the stiffening of the main-chain backbone due to the presence of these side-chain surfactants, leading to a so-called *bottle–brush* conformation, should under certain conditions be sufficient to induce lyotropic behavior in polymers that are otherwise quite flexible. That this may not be an entirely trivial matter follows from the fact that Birshtein and co-workers[8] came to the exactly opposite conclusion. According to their analysis, the persistence length of a polymer–surfactant complex increases as a function of the surfactant chain length in a way that is comparable to the increase in thickness of the complex. Since lyotropic behavior requires a large value (>10) for the ratio between persistence length and thickness, their analysis excludes such behavior. According to Fredrickson's analysis, however, the same ratio scales with the surfactant chain length to a power that is slightly larger than 1.

The influence of flexible side chains on the conformation of flexible polymers has already been studied extensively in the field of comb-shaped polymers including liquid crystalline polymers with mesogenic side groups with various lengths of the flexible chain ends (not to be confused with flexible spacers). The main results are summarized in a monograph by Platé and Shibaev.[9] The most common comb-shaped polymers discussed are the polyacrylates, polymethacrylates, polyacrylamides, and polymethacrylamides, all with alkyl side chains of varying lengths of up to 22 CH_2 units. Most of these older studies focused on confor-

† Also Laboratory of Polymer Chemistry and Materials Science Center, University of Groningen, Nijenborgh 4, 9747 AG Groningen, The Netherlands.

® Abstract published in *Advance ACS Abstracts,* September 1, 1995.

0024-9297/95/2228-7088$09.00/0

mational properties under Θ-conditions, or rather the determination of Θ-conditions, assuming the concept has any meaning for the amphiphilic polymers. Under these conditions the results suggest that the main-chain backbone is considerably stiffened but that the effect is even more pronounced for the side chains, the order parameter of which has values on the order of that of low molecular weight nematic liquid crystals. In the solid state a melting point corresponding to the melting of hexagonally ordered alkyl side chains may be observed for side chains consisting of 12 CH_2 units and more.

In an endeavor to test some of these ideas, lyotropic behavior at this stage and formation of thermoplastic interpenetrating polymer networks in a later stage, poly(2-vinylpyridine) (P2VP) and poly(4-vinylpyridine) (P4VP) were chosen as suitable model systems for flexible nonconjugated polymers. The nitrogen in the ring is a weak base and can form acid–base complexes with acidic surfactants. Dodecylbenzenesulfonic acid (DBSA) was selected as the surfactant molecule because it has a relatively long tail and it is readily available. It has also been used before in experimental studies on PANI which is a semi-rigid-rod polymer, so that our results may be compared to those studies as well.[10,11]

Experimental Section

Materials. The P2VP (M_v = 120 000) and P4VP (M_v = 44 000) polymers used to study the bulk properties of their DBSA complexes were synthesized in the Laboratory of Polymer Chemistry of the University of Groningen (The Netherlands). The molar mass of P2VP was determined by viscosimetry in methanol using $[\eta] = 1.13 \times 10^{-3} M_v^{0.73}$.[13] The molar mass of P4VP was determined by viscosimetry in ethanol using $[\eta] = 2.50 \times 10^{-4} M_v^{0.6}$.[14] The xylene solutions were prepared from P2VP and P4VP provided by Polyscience Europe GmbH. The molar masses of P2VP (M_v = 330 000) and P4VP (M_v = 49 000) were determined in DMF[13] and in absolute ethanol,[14] respectively. All polymers are of high molar mass, and the differences due to batches are not expected to play a significant role in the formation of the present mesomorphic phases. The surfactant DBSA is of laboratory purity and was obtained from Tokio Kasei. The solvents were of analysis grade.

Polymer–Surfactant Complex Preparation. P4VP and P2VP were first dried at 60 °C in vacuum for 2 days. P4VP-(DBSA)$_x$ and P2VP(DBSA)$_x$ complexes, where x denotes the number of DBSA molecules per vinylpyridine repeat unit, were prepared by dissolving P4VP or P2VP and DBSA into DMF which had first been carefully dried by 3 Å molecular sieves. The concentrations have to be small (less than ca. 5% (w/w) complex) to yield homogeneous protonation. This was observed important to achieve complexes with good solubility to xylene. DMF was evaporated on a hot plate at 80 °C. The complexes were dried at 60 °C in vacuum for 2 days and thereafter stored in a desiccator. In this study the values of x were taken to be 0.1, 0.5, 0.8, and 1.0, where the last value of x corresponds to the nominally fully protonated PVP.

Complex/xylene solutions were obtained by dissolving given amounts of the dried P4VP(DBSA)$_{1.0}$ or P2VP(DBSA)$_{1.0}$ in xylene which had been carefully dried by 3 Å molecular sieves. The mixing was performed in a hermetically closed one-screw mixer at ca. 100 °C for 15 min. As much as ca. 70–80% (w/w) of P4VP(DBSA)$_{1.0}$ can be dissolved to xylene to form clear solutions, in which case rubberlike viscous materials are formed. The samples were stored in closed bottles and analyzed shortly. It turned out that if the materials were not carefully dried, the solubility was drastically reduced, in which case it was difficult to obtain clear solutions even at concentrations of less than 1% (w/w) of complexes. Therefore, all efforts were made to work with dry materials throughout this work.

Optical Microscopy. The optical observations were carried out with a Nikon Optiphot 66 microscope in transmission polarization mode with a Linkam TMS 91 hot stage. The samples were prepared as thin films between two glass plates. To observe possible liquid crystallinity, the solutions were sheared by sliding the cover slip to achieve orientation in the samples. In bulk complexes, the temperature was scanned between 25 and 200 °C. In complex/xylene samples, the temperature was scanned only up to ca. 120 °C and the sample cell was sealed to prevent evaporation of the solvent.

X-ray Scattering. Preliminary investigations of some of the PVP(DBSA)$_x$ complexes by X-ray scattering were performed on Beam line 8.2 of the SRS at the SERC Daresbury Laboratory, Warrington, U.K. The details of the storage ring, radiation and camera geometry, and data collection electronics have been given in detail elsewhere.[12] The camera is equipped with a multiwire quadrant detector (SAXS) located 3.5 m from the sample position and a curved knife-edge detector (WAXS) that covers 120° of arc at a radius of 0.2 m. The diffraction curve from an oriented specimen of wet collagen (rat-tail tendon) was used to calibrate the SAXS detector. Because the diffraction maximum at about 3° due to the long period of the pure complexes was measurable with a WAXS setup, a comprehensive series of X-ray scattering experiments were performed at Neste Oy (Finland) by using a Diffrac D 500 diffractometer by Siemens where the 2θ range starts from as low as 2°. Measurements were made with symmetrical reflection geometry using Cu Kα radiation with a curved graphite monochromator mounted in the diffraction beam. Furthermore, preliminary SAXS experiments on P4VP(DBSA)$_{1.0}$/xylene solutions were performed at Helsinki University. The Cu Kα radiation has been monochromatized by means of a totally reflecting mirror (Huber small-angle chamber 701) and a Ni filter. The sealed Cu anode fine focus X-ray tube has been powered by a Siemens Kristalloflex 710 H unit. The scattered radiation has been detected by a linear one-dimensional position-sensitive proportional counter (MBraun OED-50M). A narrow slit was implemented before the sample to minimize background scattering. The primary beam is narrow (fwhm ≤ 0.002 Å^{-1}) compared to its length (fwhm ≈ 0.32 Å^{-1}) at the sample. Together with the detector height profile the fwhm of the instrumental function was 0.52 Å^{-1}. The instrumental broadening was corrected by an iterative desmearing procedure.[15]

Infrared Spectroscopy. Infrared spectra of PVP(DBSA)$_x$ samples were obtained using a Nicolet 730 FT-IR spectrometer with a Nic-Plan IR microscope. Samples were prepared by DMF casting directly onto zinc selenide crystals followed by evaporation at 80 °C and drying in vacuum at 60 °C for several hours. It turned out to be difficult to remove DMF totally from the samples due to its strong hydrogen-bonding ability. Therefore, some characteristic DMF peaks may still be observable especially in samples with low levels of protonation.

Results and Discussion

In a recent paper Fredrickson[7] suggested an exciting possibility to yield flexible nonconjugated polymers which exhibit nematic order by a proper choice of surfactant and solvent molecules. According to the mechanism proposed, surfactants which bind strongly to specific sites along the backbone of flexible polymers may, under good solvent conditions with respect to the tail of the surfactants, induce sufficient rigidity in the complex formed. Essential parameters are the number of binding sites, the binding energies, and the length of the side-chain surfactant M. For a given M, the number of bound surfactant molecules per backbone monomer of the polymer, σ, determines the stiffness of the complex. At the high coverage limit the persistence length λ of the complex is predicted to vary like

$$\lambda \propto a\sigma^{17/8} M^{15/8} \quad (1)$$

where a is the Kuhn segment size (in his analysis, for simplicity, it is assumed to be the same for polymer and

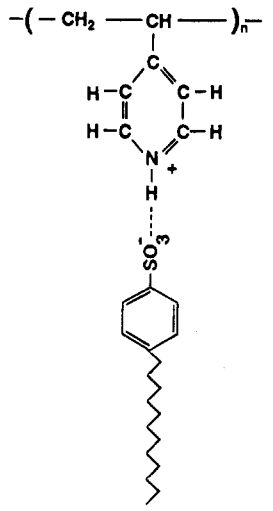

Figure 1. Protonation of poly(4-vinylpyridine) with *p*-dodecylbenzenesulfonic acid.

surfactant). The thickness of the polymer–surfactant complex R is predicted to scale like

$$R \propto a\sigma^{1/4}M^{3/4} \quad (2)$$

As a consequence the ratio λ/R, determining the possibility of lyotropic behavior, scales as

$$\lambda/R \propto \sigma^{15/8}M^{9/8} \quad (3)$$

In order to observe lyotropic behavior, this ratio should, according to an analysis by Khokhlov and Semenov,[16] exceed 10, which taken at face value would also require the side chains to consist of on the order of 10 flexible units provided $\sigma \cong 1$.

The authors of ref 8 found the same relation (2) for the thickness of the polymer–surfactant complex. However, their analysis of the rigidity of a stretched chain leads to the conclusion that bending does not increase the free energy since the "grafted" chains are redistributing partly in the bending process moving from the concave to the convex side. Since Fredrickson did take redistribution into account, and in a more sophisticated manner, we proceed from the assumption that lyotropic behavior is a real possibility.

In our case the main chain is either P4VP or P2VP and the side-chain surfactant is DBSA. Figure 1 presents a schematic picture of the repeat unit of the P4VP(DBSA)$_{1.0}$ complex, i.e., at full protonation. Assuming this can be realized, the above discussion, leading to expressions with unknown front factors, demonstrates that a side chain of the length of DBSA can, in principle, be long enough to induce lyotropic behavior. Since the number of bound surfactant molecules is extremely important in this respect, this will be discussed first.

FT-IR Analysis. With respect to protonation and associations, the most important feature of the spectra is the band at ca. 900 cm^{-1} in pure DBSA corresponding to $-SO_3H$, which on protonation is replaced by a band due to SO_3^- at ca. 1200 cm^{-1}. Additional FT-IR features of interest have been considered recently in relation to polymer blends of poly(vinylpyridines) with other polymers containing hydroxyl groups that form hydrogen bonds with the basic nitrogen.[17,18] Studies of infrared spectra of pyridine hydrogen bonded with alcohols[19] and of interpolymer P2VP/poly(ethylene-*co*-methacrylic acid) complexes[20] demonstrate that the most affected bands

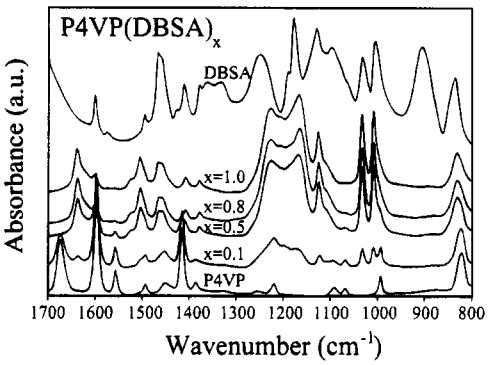

Figure 2. Infrared spectra of P4VP(DBSA)$_x$ (x = 0.1, 0.5, 0.8, 1.0), P4VP, and DBSA.

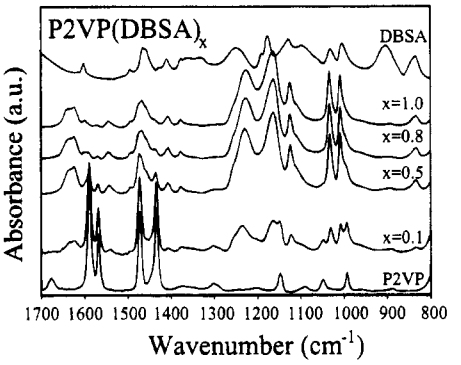

Figure 3. Infrared spectra of P2VP(DBSA)$_x$ (x = 0.1, 0.5, 0.8, 1.0), P2VP, and DBSA.

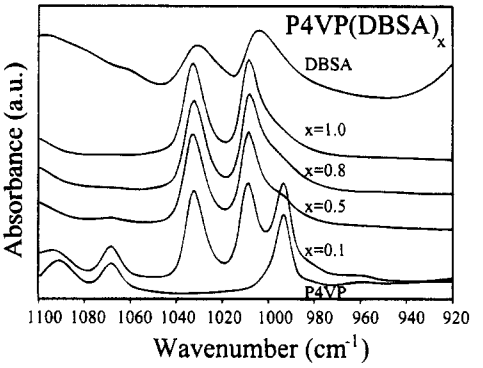

Figure 4. Infrared spectra in the 900–1100 cm^{-1} region for P4VP(DBSA)$_x$ (x = 0.1, 0.5, 0.8, 1.0), P4VP, and DBSA.

of the poly(vinylpyridines) are those concerned with stretching modes of the pyridine ring: 1590, 993, and 625 cm^{-1} for P2VP and 1597, 993, and 627 cm^{-1} for P4VP. On formation of hydrogen bonds, these bands shift to higher frequencies. In our case proton transfer rather than hydrogen bonding is expected to take place. The most affected bands remain the same, however, and the effect is only expected to be larger. Figure 2 presents the spectra for P4VP(DBSA)$_x$, x = 0.1, 0.5, 0.8, 1.0, together with the pure polymer and DBSA. Figure 3 presents the corresponding spectra for P2VP. Figures 4 and 5present a detailed picture of the 1000 and 1600 cm^{-1} region for the P4VP samples; Figures 6 and 7 do the same for P2VP.

Figures 2 and 3 show that the $-SO_3H$ band of DBSA at 900 cm^{-1} has completely disappeared from all the samples where poly(vinylpyridine) is complexed with DBSA. Instead, a very pronounced broad band around 1200 cm^{-1} has appeared, demonstrating complete proton transfer. Furthermore, Figures 4 and 6 demonstrate that the band at 993 cm^{-1} of the pure polymers

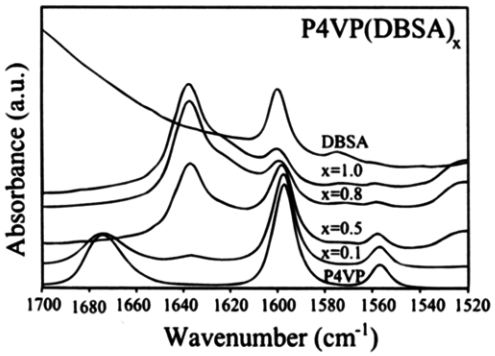

Figure 5. Infrared spectra in the 1500–1700 cm^{-1} region for P4VP(DBSA)$_x$ (x = 0.1, 0.5, 0.8, 1.0), P4VP, and DBSA.

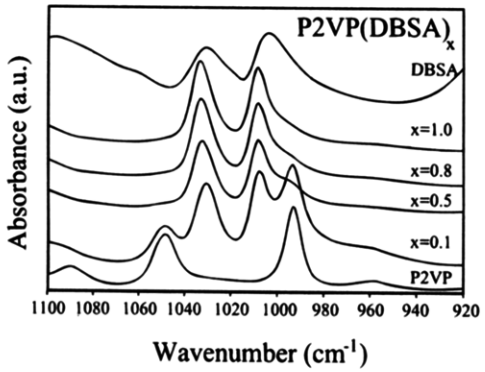

Figure 6. Infrared spectra in the 900–1100 cm^{-1} region for P2VP(DBSA)$_x$ (x = 0.1, 0.5, 0.8, 1.0), P2VP, and DBSA.

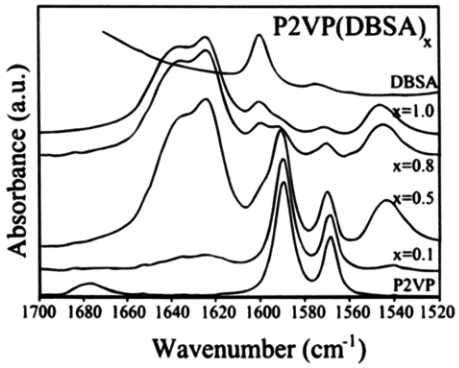

Figure 7. Infrared spectra in the 1500–1700 cm^{-1} region for P2VP(DBSA)$_x$ (x = 0.1, 0.5, 0.8, 1.0), P2VP, and DBSA.

disappears completely on full protonation. It is replaced by two bands of similar strength at 1008 and 1033 cm^{-1}. Moreover, Figure 5 demonstrates the appearance of a very strong band at 1637 cm^{-1} in the protonated P4VP samples, replacing the 1597 cm^{-1} band of pure P4VP. The former corresponds to the formation of pyridinium replacing the pyridine. The remaining peak at 1600 cm^{-1} is due to the benzene ring of DBSA. Furthermore, the small peak at 1674 cm^{-1} in pure P4VP and in P4VP-(DBSA)$_{0.1}$ corresponds to DMF not being completely removed from these largely unprotonated samples obviously due to its large hydrogen-bonding capability. Figure 7 demonstrates a slightly different behavior for the P2VP samples. Here the pyridine band is at 1590 cm^{-1} and can be distinguished clearly from the 1600 cm^{-1} band of DBSA. The pyridine band is almost, but not completely, removed for P2VP(DBSA)$_{1.0}$. The main difference, however, is the appearance of a pronounced double peak at 1636 and 1624 cm^{-1}, whereas in the P4VP samples the 1624 cm^{-1} peak is hardly observable. A straightforward explanation for this difference is not known to us. The small peak at 1674 cm^{-1} corresponds again to traces of DMF.

Figure 8. Polarized optical microscopy picture of a 60/40 (w/w) P4VP(DBSA)$_{1.0}$/xylene sample at room temperature sheared by sliding the cover slip.

A bottle–brush conformation requires the condition $\sigma \gg M^{-3/5}$ to be satisfied. In our case the FT-IR data demonstrate convincingly that, as in the case of PANI/CSA, the equilibrium between poly(vinylpyridine) and DBSA is shifted completely to protonation. The coverage of the main-chain backbone is therefore limited by the number of binding sites available. Saturation occurs at a molar ratio of 1:1 DBSA to vinylpyridine repeat units of P2VP and P4VP, respectively, which clearly satisfies the above condition.

Optical Microscopy. Polarized optical microscopy showed that the fully DBSA protonated P4VP and P2VP are birefringent from room temperature at least to 200 °C, indicating liquid crystalline order. The same phenomena were observed when the degree of protonation was reduced from x = 1.0 to 0.8 and 0.5. As could be excepted, x = 0.1 is completely isotropic, thus resembling the atactic unprotonated polymers. To determine lyotropic behavior in solution, the poly(vinylpyridine)–DBSA complexes were dissolved in xylene, a good solvent for the alkyl side chain (Mark–Houwink exponent 0.8 for polyethylene). Polarization microscopic observations were used to preliminarily determine the phase diagram. For the fully protonated P4VP, lyotropic behavior was found if the concentration of xylene was less than 50% (w/w). Figure 8 shows an example of birefringent texture of 60/40 (w/w) P4VP(DBSA)$_{1.0}$/xylene under polarized microscopy obtained by shearing the sample by sliding the cover plate. The samples were investigated as a function of temperature from room temperature up to 125 °C. At a concentration of xylene of 50% (w/w), liquid crystallinity is only present near room temperature; at lower xylene concentration lyotropic behavior was observed at all investigated temperatures. In contrast, the P2VP(DBSA)$_{1.0}$ samples became birefringent only at xylene concentrations of 30% (w/w) and lower. For both xylene concentrations of 30 and 20% (w/w), liquid crystallinity was observed only near room temperature. Therefore, it seems clear that, in the fully protonated condition, P4VP is more favorable than P2VP to produce lyotropic solutions in xylene. Although it is hard to pin down the precise mechanism leading to this difference, clearly the *ortho* position of P2VP is more difficult to access for the surfactant than the *para* position of P4VP. The position

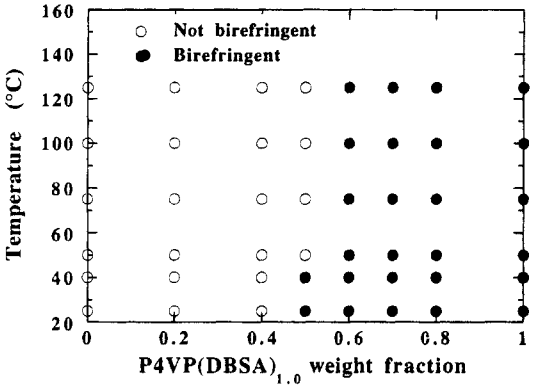

Figure 9. Phase diagram of P4VP(DBSA)$_{1.0}$/xylene.

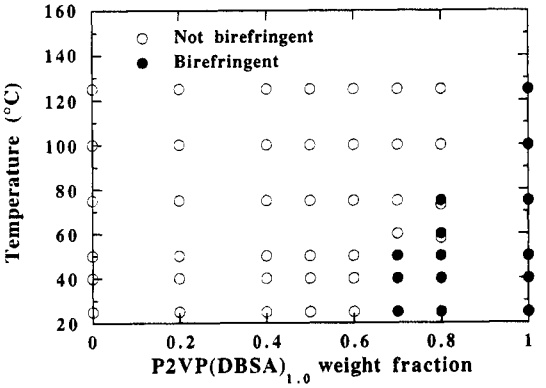

Figure 10. Phase diagram of P2VP(DBSA)$_{1.0}$/xylene. Note the limiting cases in the data of 80/20 (w/w).

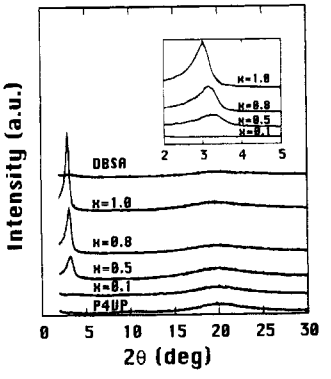

Figure 11. WAXS data for P4VP(DBSA)$_x$ (x = 0.1, 0.5, 0.8, 1.0), P4VP, and DBSA. The small-angle region is shown in the inset in more detail.

of DBSA in the case of P2VP seems to be less favorable for mesomorphic structures, a fact that is corroborated by the X-ray scattering data that will be discussed next. Figures 9 and 10 present the phase diagrams obtained by the birefringence measurements.

X-ray Scattering. To obtain information about the mesomorphic structure of the poly(vinylpyridine)–DBSA complexes, X-ray scattering experiments were first performed on solvent-free samples. The observed diffraction curves at small scattering angles are shown in Figures 11 and 12. As can be seen, for 0.5, 0.8, and 1.0 cases, a strong diffraction maximum is present at approximately $2\theta = 3°$. The characteristics of the X-ray diffraction curve are very similar to results published some years ago by Lipatov and co-workers[21,22] on liquid crystalline polymers with phenyl benzoate side groups with various lengths of flexible chain ends ($C_{12}H_{25}$ and $C_{16}H_{33}$, respectively). There the diffraction maximum is argued to be due to a layer structure characterized

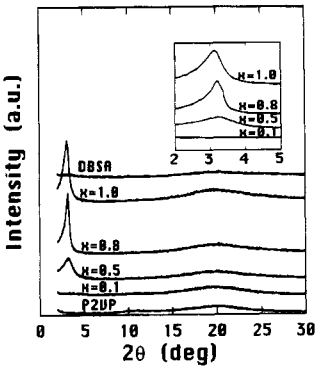

Figure 12. WAXS data for P2VP(DBSA)$_x$ (x = 0.1, 0.5, 0.8, 1.0), P2VP, and DBSA. The small-angle region is shown in the inset in more detail.

Table 1. Long Period d, Average Domain Size D, and the Estimated Number of Layers for P4VP(DBSA)$_x$ and P2VP(DBSA)$_x$ (x = 0.5, 0.8, 1.0)

	x	d (Å)	domain size (Å)	no. of layers
P4VP	0.5	27.0	146	6
	0.8	27.6	204	8
	1.0	29.3	260	9
P2VP	0.5	27.4	100	5
	0.8	27.3	238	10
	1.0	28.2	180	7

by an imperfect one-dimensional order normal to the layers. Their analysis in terms of the one-dimensional correlation function demonstrated that the absence of second-order diffraction maxima is due to the correlation in the packing being restricted to approximately five adjacent layers of polymers. A very recent example, which resembles even closer our system, involves polyelectrolyte–surfactant complexes of poly(styrenesulfonate) and different backbone alkyltrimethylammonium derivatives studied by Antonietti and coworkers.[23] Also there the mesomorphic layer structures are characterized by a single diffraction maximum. Assuming a layer structure in our case as well, a long period d can be derived using Bragg's law. The results are summarized in Table 1 (applying Lorentz correction has only a very small effect on the absolute values). For P4VP, d decreases from 29.3 Å at full protonation to 27.0 Å for x = 0.5. These values indicate that the alkyl side chains are considerably stretched, with a large amount of interdigitation between the side chains from the poly(vinylpyridine) chains in neighbouring layers. The relatively small decrease for lower values of σ indicates that the backbone as well as the side chains become progressively less stretched. Figure 13 presents the long period as a function of the amount of DBSA, and assuming tentatively a linear dependence implies that the long period extrapolates to approximately 24 Å at zero concentration of DBSA. Since, this cannot possibly have any relation with the thickness of the hydrophilic layer, it suggests that at low concentrations of DBSA only small parts of different chains of a somewhat higher than average degree of protonation segregate in small domains with a mesomorphic structure. This agrees with the observation that the diffraction maxima become progressively broader and of lower intensity. The mean size of the ordered domains D can be related to the broadening of the diffraction maxima by Scherrer's equation

$$D = K\lambda/(L \cos \theta) \quad (4)$$

where L is the pure X-ray diffraction breadth free of all

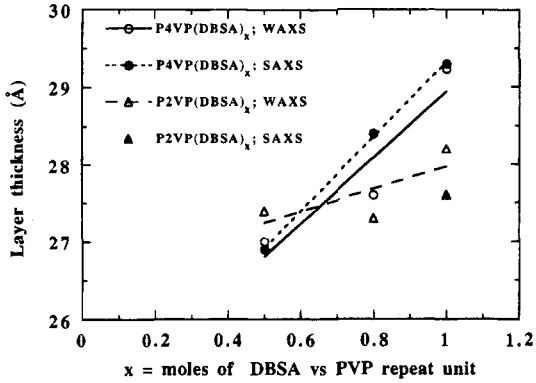

Figure 13. Long period d for P4VP(DBSA)$_x$ and P2VP(DBSA)$_x$ as a function of x. SAXS results are from Daresbury, and WAXS, from Neste.

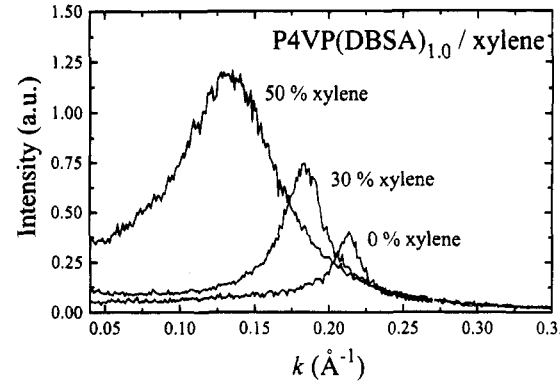

Figure 14. SAXS data for P4VP(DBSA)$_{1.0}$ in xylene solution (0, 30, 50% (w/w) xylene).

broadening due to the experimental method employed in observing it. λ is the wavelength, 2θ the scattering angle, and K a constant approximately equal to 0.94 in our case. On the basis of this equation, the domain size of the P4VP samples is calculated to decrease from 260 Å at full protonation to 146 Å at 50% protonation (cf. Table 1). Hence, the domain size decreases roughly from 9 to 6 layers. The small number of layers of the correlated domains combined with random fluctuation in their spacing could explain the absence of higher order diffraction maxima. Another possible explanation has been suggested by Antonietti et al.[23] for their systems, which invoke layers with different electron densities.

For P2VP, the situation is similar, but with some striking differences as well. The long period d equals 28.2 Å at full protonation instead of the value of 29.3 Å for P4VP. This smaller value seems, given the different position of the nitrogen atom, quite reasonable. The long period is found to be less sensitive to a decreasing amount of DBSA (cf. Figure 13), but this may also be related to the fact that the domain size is predicted to have an optimum near $x = 0.8$ rather than at full protonation. It suggests that fully protonated P2VP–DBSA complexes have conformations that fit less well in layered structures, something which the birefringence measurements also clearly demonstrated.

Our mesomorphic structures resulting from flexible poly(vinylpyridine) polymers protonated by DBSA can be compared with those obtained using more rigid polymers. In semi-rigid-rod polyaniline fully protonated and plasticized with DBSA, mesomorphic structure was observed with a layer thickness of 27.3 Å.[11] Mesomorphic structures of polypyrrole–surfactant complexes have been reported by Wegner.[24] One has to point out, however, that, in these cases, the mesomorphic behavior could be much more anticipated than in the flexible polymers and therefore the underlying physics may be different.

A layered structure for the melt differs considerably from the nematic type order of cylindrical symmetric rigid bottle brushes. However, the predictions about this latter type of ordering are explicitly for good solvent conditions, where the excluded-volume effect induces sufficient rigidity to the complex. Although we can not at present exclude the possibility that the anisotropic phase in xylene is of the nematic type, it seems not unreasonable to expect that xylene is merely preferentially diluting the hydrophobic alkyl side-chain layers. Preliminary SAXS experiments on P4VP(DBSA)$_{1.0}$/xylene mixtures of 70/30 and 50/50 (w/w) presented in Figure 14 indicate that the long period increases from 29.4 Å for the pure complex to about 34.3 Å at 30% (w/w) xylene and further to about 47.5 Å at 50% (w/w) xylene. The relatively small increase from 29.4 to 34.4 Å can only be explained by preferential solvation of the hydrophobic layer if at the same time the hydrophobic layer increases its size also in a direction parallel to the layer. In other words, this result implies that the hydrophilic layer has to stretch in a direction parallel to the layer as well, which in turn implies that the polymeric backbones have to stretch. But, as discussed in the beginning, this is exactly what should be expected for bottle–brush type conformations in a good solvent for the side chains. The further increase to 47.5 Å corresponds approximately to the additional amount of solvent; no further stretching of the backbones has to be invoked. The estimated domain sizes are shown in Table 2. It shows that increasing the weight fraction of xylene reduced the domain sizes. For example, at 50% (w/w) xylene, only two layers are incorporated.

Table 2. Long Period, Average Domain Size D, and the Estimated Number of Layers for Different Weight Fractions of P4VP(DBSA)$_{1.0}$ in Xylene

P4VP(DBSA)$_{1.0}$ (w/w %)	$2\pi/k$ (Å)	D (Å)	no. of layers
100	29.4	260	8
70	34.4	170	6
50	47.5	80	2

Concluding Remarks

The central theme of the present work concerns the possibility of inducing bottle–brush type conformations into flexible nonconjugated polymers. P4VP and P2VP complexed with DBSA were taken as model systems, and both exhibited lyotropic behavior in xylene, a good solvent for the alkyl side chain. On the basis of the X-ray diffraction data, the ordered domains are shown to encompass on the order of 5–10 layers only. In solution, the poly(4-vinylpyridine)–DBSA complexes remain birefringent up to 50% (w/w) of the xylene solvent. The presence of mesomorphic structures under these conditions has been verified with SAXS, and these results suggest that the mesomorphic structures could be present at still lower concentrations of the complex in spite of the fact that optical microscopy did not show birefringence anymore. The scattering data demonstrate that the poly(4-vinylpyridine) backbones stretch on the addition of xylene. Therefore, although we expect it to remain a layered structure rather than a nematic solution of stiff cylinders, the excluded-volume effect of the side chains is manifestly present.

Future work will involve a more thorough small-angle X-ray scattering study on the complexes in solution.

Furthermore, detailed molecular modeling of the polymer complex conformations will be undertaken. In this way we ultimately hope to be able to rationalize the differences observed between P2VP and P4VP and find out more about the rigidity induced by these types of surfactants. Another important aspect and clearly related to the molecular modeling concerns the tacticity of the polymers. Future work will include tactic poly(vinylpyridines) as well.

Finally, the possibility of preparing percolating structures of P4VP(DBSA) and P2VP(DBSA) in polyolefin matrices or in other matrices employing appropriate surfactants, much like PANI(CSA) in polar matrices, at low concentrations of the complex will be explored. In particular, the possibility of using less than a stoichiometric amount of DBSA could be of interest. The remaining, not protonated, weakly basic nitrogens in the rings may keep the system useful for various applications.

Acknowledgment. The authors are grateful for Alpo Toivo, Maarit Taka, Heidi Österholm, and Helena Leuku of Neste Oy (Finland) for FT-IR and WAXS analysis. Lizette Oudhuis (University of Groningen) and Wim Bras (SERC) are acknowledged for assistance during the SAXS measurements at Daresbury. The authors have benefited from numerous discussions with Lars-Olof Pietilä and Lisbeth Ahjopalo of VTT Chemical Technology (Finland). This work was supported by grants from Finnish Academy, Technology Development Centre (Finland), and Neste Oy Foundation.

References and Notes

(1) Cao, Y.; Smith, P. *Polymer* **1993**, *34*, 3139.
(2) Yang, C. Y.; Cao, Y.; Smith, P.; Heeger, A. J. *Synth. Met.* **1993**, *53*, 293.
(3) Laradji, M.; Mouritsen, O. G.; Toxvaerd, S.; Zuckermann, M. J. *Phys. Rev. E* **1994**, *50*, 1243.
(4) Park, D.-W.; Roe, R.-J. *Macromolecules* **1991**, *24*, 5324.
(5) Balberg, I. *Philos. Mag. B* **1987**, *56*, 991.
(6) Ikkala, O. T.; Pietilä, L.-O.; Ahjopalo, L.; Österholm, H.; Passiniemi, P. J. *J. Chem. Phys.*, submitted.
(7) Fredrickson, G. H. *Macromolecules* **1993**, *26*, 2825.
(8) Birshtein, T. M.; Borisov, O. V.; Zhulina, Ye. B.; Khokhlov, A. R.; Yurasova, T. A. *Polym. Sci. U.S.S.R.* **1987**, *29*, 1293.
(9) Platé, N. A.; Shibaev, V. P. *Comb-Shaped Polymers and Liquid Crystals*; Plenum Press: New York and London, 1987.
(10) Cao, Y.; Smith, P.; Heeger, A. J. *Synth. Met.* **1992**, *48*, 91.
(11) Kärnä, T.; Laakso, J.; Savolainen, E.; Levon, K. European Patent Application EP 0 545 729 A1, 1993.
(12) Bras, W.; Derbyshire, G. E.; Ryan, A. J.; Mant, G. R.; Felton, A.; Lewis, R. A.; Hall, C. J.; Greaves, G. N. *Nucl. Instrum. Methods Phys. Res.* **1993**, *A326*, 587.
(13) Arichi, S. *Bull. Chem. Soc. Jpn.* **1966**, *39*, 439.
(14) Berkowitz, J. B.; Yamin, M.; Fuoss, R. M. *J. Polym. Sci.* **1958**, *28*, 69.
(15) Lake, J. *Acta Crystallogr.* **1967**, *23*, 191.
(16) Khokhlov, A. R.; Semenov, A. N. *J. Stat. Phys.* **1985**, *38*, 161.
(17) Cesteros, L. C.; Meaurio, E.; Katime, I. *Macromolecules* **1993**, *26*, 2323.
(18) Cesteros, L. C.; Isasi, J. R.; Katime, I. *Macromolecules* **1993**, *26*, 7256.
(19) Takahashi, H.; Mamola, K.; Plyler, E. K. *J. Mol. Spectrosc.* **1966**, *21*, 217.
(20) Lee, J. Y.; Painter, P. C.; Coleman, M. M. *Macromolecules* **1988**, *21*, 954.
(21) Shilov, V. V.; Tsukruk, V. V.; Bliznyuk, V. N.; Lipatov, Yu. S. *Polymer* **1982**, *23*, 484.
(22) Shilov, V. V.; Tsukruk, V. V.; Lipatov, Yu. S. *J. Polym. Sci., Polym. Phys. Ed.* **1984**, *22*, 41.
(23) Antonietti, M.; Conrad, J.; Thünemann, A. *Macromolecules* **1994**, *27*, 6007.
(24) Wegner, G. *Makromol. Chem., Macromol. Symp.* **1986**, *1*, 151.

MA9506546